Design and Performance Evaluation of a Minimally Invasive Telerobotic Platform for Transurethral Surveillance and Intervention

Roger E. Goldman, Andrea Bajo, Lara S. MacLachlan, Ryan Pickens, S. Duke Herrell, Nabil Simaan

***Abstract*—Bladder cancer, a significant cause of morbidity and mortality worldwide, presents a unique opportunity for aggressive treatment due to the ease of transurethral accessibility. While the location affords advantages, transurethral resection of bladder tumors can pose a difficult challenge for surgeons encumbered by current instrumentation or difficult anatomic tumor locations. This paper presents the design and evaluation of a telerobotic system for transurethral surveillance and surgical intervention. The implementation seeks to improve current procedures and enable development of new surgical techniques by providing a platform for intravesicular dexterity and integration of novel imaging and interventional instrumentation. The system includes a dexterous continuum robot with access channels for the parallel deployment of multiple visualization and surgical instruments.**

The paper first presents the clinical conditions imposed by transurethral access and the limitations of the current state-of-the-art instrumentation. Motivated by the clinical requirements, the design considerations for this system are discussed and the prototype system is presented. Telemanipulation evaluation demonstrates submillimetric RMS positioning accuracy and intravesicular dexterity suitable for improving transurethral surveillance and intervention.

***Index Terms*—Surgical Robotics, Transurethral Resection of Bladder Tumor, Telemanipulation, Dexterity Enhancement**

I. Introduction

URINARY bladder cancer is a significant cause of patient morbidity and mortality, accounting for an estimated 73,510 new cases and 14,880 cancer-related deaths in the United States in 2012 [1]. Transurethral resection (TUR) coupled with pathological staging are essential procedures for diagnosis and treatment of primary and recurrent nonmuscle-invasive bladder cancer (NMIBC) [2]–[4]. Despite the significant literature and clinical history of the TUR procedure in treatment of bladder cancer, outcomes are variable and highly dependent on the experience and technical ability of the urologic surgeon. The limitations of the current instrumentation play a critical role in the ability of surgeons to deliver consistent care [5].

R. Goldman is with the College of Physicians and Surgeons, Columbia University, New York, NY 10032 USA, email: reg2117@columbia.edu.

L. MacLachlan is with the Department of Urology, Columbia University, New York, NY 10027 USA, email: ls2574@columbia.edu

R. Pickens and D. Herrell are with the Department of Urology, Vanderbilt University, Nashville, TN, USA, email: {ryan.pickens,duke.herrell}@vanderbilt.edu

A. Bajo and N. Simaan are with the Department of Mechanical Engineering, Vanderbilt University, Nashville, TN 37240 USA email: {andrea.bajo,nabil.simaan}@vanderbilt.edu

Manuscript received June 1, 2012; revised August 25, 2012.

Incremental advances have been made toward improving instrumentation for TUR procedures [6], but the fundamental approach and the form factor has not significantly changed since the early 1930s. Advancement in the instrumentation to provide improved visualization, increased manipulation precision and intravesicular dexterity can potentially yield significant improvements in TUR techniques and patient outcomes.

The advent of computer controlled technology has facilitated significant advancements in the general field of urology through improvements to the positioning accuracy, repeatability and dexterity of surgical instrumentation. Babbar and Hemal [7] review the state of the art in percutaneous urologic surgical procedures, noting robot assistance has gained wide acceptance in prostatectomy, cystectomy and nephrectomy. Research platforms for image guided brachytherapy have also shown initial success. Goldenberg et al. [8], Tokuda et al. [9], and Mozer et al. [10] present and review various robotic systems for guidance of needle placement with parallel real-time fluoroscopy, magnetic resonance imaging or computed tomography imaging.

Improvement of the instrumentation for transurethral procedures has been an area of active interest in clinical and engineering research groups. Sánchez de Badajoz et al. [11], [12] reported a master-slave system for controlling a commercial rigid resectoscope. Hashimoto et al. [13] presented a slave manipulator for transurethral prostate resection. Aron and Desai [14] proposed adaptation of a commercial robotic catheter system for direct visualization and treatment of stones and tested the system in an eighteen patient clinical feasibility trial. Pantuck et al. [6] described an iteration to the cautery element of a resectoscope and evaluated the device in a multi-center clinical trial for safety and efficacy without complications. Jong Yoon et al. [15] reported a shape memory alloy actuated mechanism for automated surveillance of the bladder urothelium. Despite this active research, no system exists for simultaneously adding precision and intravesicular dexterity to the resection technique while providing a platform for deploying new imaging techniques in parallel to traditional wire and laser tumor resection instruments.

The contribution of this work is presentation and evaluation of a novel telerobotic platform for transurethral inspection of bladder urothelium and tumor resection. The aims of the system are toward improving and expanding the repertoire of techniques for urologic surgeons, improving surgical resection accuracy and surveillance coverage, and deploying and evaluating novel imaging techniques for TUR. In this paper,

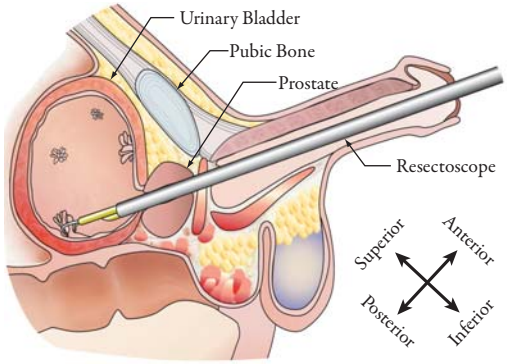

Fig. 1. Overview of TURBT Procedure. The resectoscope is inserted through the urethra to access the bladder. Tumors in the bladder wall must be resected through to the muscular layer of the bladder. Motion of the resectoscope is limited by the soft tissue and pubis anterior-superiorly and posterior-inferiorly. Medial and lateral motion is further hampered by the patients legs.

we demonstrate a system capable of delivering simultaneous visualization and precision resection in a surgical system that can be rapidly deployed transurethrally with little change to the current cystoscopy workflow.

II. Clinical Motivation and Requirements

TUR procedures provide incisionless natural orifice access to the bladder urothelium via the urethra as depicted in Fig. 1. TUR of bladder tumors (TURBT) serves dual therapeutic and diagnostic roles. A surgeon performs a TURBT procedure to resect all visibly diseased or suspect tissue with adequate margins while providing samples for pathologic analysis and simultaneously estimating the level of invasiveness of malignant tissue for clinical staging [3], [16], [17].

The modern instrument for TURBT procedures is the urologic resectoscope. The device consists of multiple telescoping and interlocking parts. An outer and inner sheath interlock and serve to define the location and orientation of the resectoscope in the urethra and bladder. The sheaths additionally provide channels for the continuous circulation of fluid. Continuous fluid circulation is required for adequate visualization and maintenance of optimal bladder filling [18]. A "working element," which guides various interchangeable monopolar electrocautery attachments or fiber-optic conduits for therapeutic laser energy, locks into the inner diameter of the inner sheath. Linear advancement of the working element with respect to the interlocking sheaths is controlled by handles on the proximal end of the working element. An endoscope, inserted through the working element, provides visualization.

During the TURBT procedure, the resectoscope is inserted through the urethra and the urothelium is inspected for macroscopic signs of change to the tissue structure, Fig. 1. Samples are taken at visible lesions and benign areas for pathologic analysis. Subsequently, all visible lesions and suspicious tissue are removed. The benefits of the procedure are contrasted to open or percutaneous procedures for muscle-invading bladder cancers which require more drastic care, including complete resection of the bladder and adjuvant systemic chemotherapy.

Visualization during TURBT is the most important clinical tool for documenting tissue abnormalities. Direct white-light based visualization, termed cystoscopy, serves as the gold standard for surveillance of bladder cancer recurrence. Despite the role as a clinical standard, experimental evaluation of cystoscopy has demonstrated widely varying reliability. False negative diagnosis rates of up to 30% were reported during routine cystoscopy [19]–[21]. Additionally, surface imaging is insufficient for accurately locating the margins of tumors with underlying finger-like submucosal invasion which may be hidden beneath benign urothelium [3]. Recently, parallel imaging techniques, such as narrow band imaging (NBI), optical coherence tomography and photodynamic diagnosis (PDD) have been proposed to improve the sensitivity and specificity of surveillance [4], [22]. A method for deployment of these novel imaging techniques during TURBT procedures, in addition to reducing the complexity of cystoscopy, will enable complete clinical diagnosis, staging and resection.

Tumor resection of NMIBC is technically challenging because of the requirements for high precision while following the complex curve of the bladder during resection [18]. An electrocautery loop wire is used to progressively remove tumor and bladder wall through successive thin cuts. Depending on intravesicular pressure, lesion location and inflammation of tissue, the bladder wall thickness varies from less than 3 mm to greater than 13 mm [23]–[25]. Submillimetric precision during resection passes is required to avoid perforation. Maneuverability of the instrumentation can be severely limited by anatomic constraints of the pelvis and adequate visualization may be hampered by the significant bulk of tissue constraining the instrumentation at the insertion site as depicted in Fig. 1.

The technical challenges of manual TURBT procedures are associated with considerable clinical ramifications. Despite recommendations to perform complete resection of all visible tumors during an initial TURBT, a study of 150 consecutive patients with NMIBC undergoing repeat transurethral resection within six weeks of the initial procedure found 76% with residual tumor [3]. Perforations in the bladder due to full wall resection or damage deep enough to the bladder exterior has been noted in studies at up to 5% of all TUR procedures [3], [18]. In a multi-center prospective study, high variability in the quality of the resection has been noted and attributed to variability in surgeon technique [26].

Ukai et al. [27] further suggested the lesion location influences resectability. In certain areas of the bladder, the ideal angle of approach to a tumor may be kinematically infeasible such that the bladder wall cannot be appropriately reached or traced. The anatomic constraints of the entrance through the urethra make access to anterior regions of the bladder difficult or infeasible without external manipulation. Wilby et al. [5] have attributed instrumentation as a significant limitation influencing resection quality.

Given the limitations of current instrumentation, improvement of the basic tools of the TURBT presents significant potential to reduce the complexity of the procedures, reduce perioperative and postoperative complications and improve patient outcomes.

III. System Design

A viable alternative to the standard urologic resectoscope must meet the clinical requirements of the current TURBT

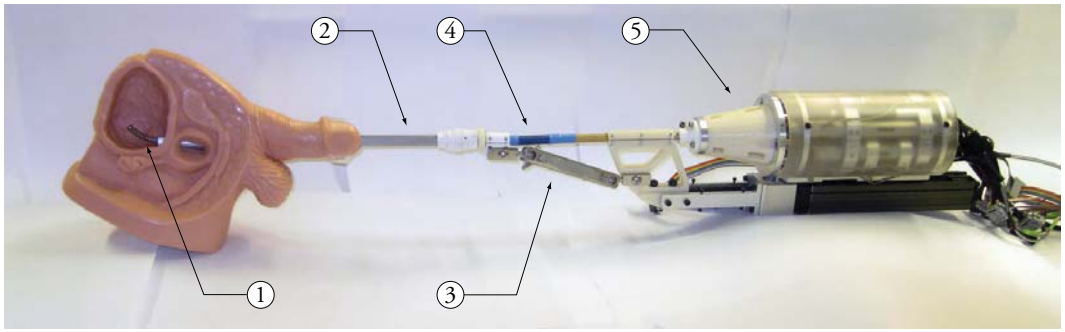

Fig. 2. Surgical Slave System coupled to a standard urologic resectoscope. ① Distal Dexterous Manipulator, ② Resectoscope Mockup, ③ Manual adjustment arm, ④ Flexible section, ⑤ Actuation Unit

procedures while extending the capabilities for improvement of current techniques and for development of novel procedures. The proposed design for transurethral telerobotic system is composed of a simple master interface for remote operator control and a slave system for direct interaction and intervention with a patient. The design choices prescribed by the clinical demands and a description of the system components are presented in the following sections.

A. Robotic Surgical Slave System

The ultimate goal of the robotic slave system is delivery of intravesicular visualization and dexterous instrumentation. To meet these requirements, a novel slave system was designed and constructed as presented in Fig. 2. The surgical slave robot consists of a distal dexterous manipulator providing intravesicular dexterity ①, a system for coupling to and stabilizing a standard urologic resectoscope ② (a model of the resectoscope with geometric specifications and the proximal coupling equivalent to standard resectoscope sheaths is shown in the figure), and an actuation unit with force sensing capability ⑤ for detection of contact [28], force sensing [29], [30] and compliant motion control [31]. Maintaining compatibility with the sheaths of the resectoscope allows fluid recirculation with instrumentation readily available in the cystoscopy suite. The slave robot also incorporates a manual adjustment arm ③ and a flexible shaft section ④ for rapid system deployment and for minimizing disruption to clinical work flow when device removal or readjustment is necessary. Details of these subsystems are introduced below.

1) Distal Dexterous Manipulator: The distal dexterous manipulator (DDM) provides intravesicular dexterity by allowing fine motion and positioning decoupled from the motion of the introducing resectoscope. Distal dexterity fulfils several purposes: it facilitates surveillance and surgical intervention in difficult to reach areas of the bladder; it obviates the need for using suprapubic pressure to reach anterior aspects of the bladder (thus reducing the need for patient-side assistance); and it provides control of the angle of approach with respect to interior walls of the bladder in a manner not achievable using existing straight instruments. The overall performance specifications of the DDM are designed to meet the operative challenges of intravesicular intervention. The DDM achieves a reachable workspace exceeding the volume of a ⌀40 mm sphere, which is approximately equivalent to a moderately sized, 300 mL, bladder [32]. As will be demonstrated in the experimental sections, the end effector provides sub-millimetric positioning accuracy.

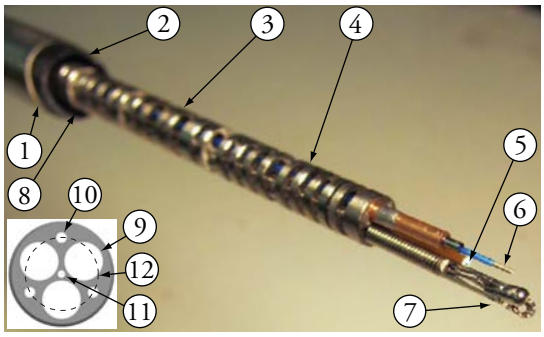

Fig. 3. Photograph of the surgical slave distal dexterous manipulator (DDM). ① Resectoscope outer sheath, ② Resectoscope inner sheath, ③ Proximal continuum segment, ④ Distal continuum segment, ⑤ Fiberscope, ⑥ Laser cautery fiber, ⑦ Biopsy forceps, ⑧ Insertion tube. Inset depicts a cross section of the DDM disks. ⑨ Instrumentation channels, ⑩ Secondary backbone lumen, ⑪ Primary backbone lumen, ⑫ Pitch circle

The DDM shown in Fig. 3 is composed of proximal ③ and distal ④ serially-stacked continuum segments. Each segment uses one centrally located passively bending primary backbone and three actuated secondary backbones. The secondary backbones are circumferentially distributed along a pitch circle with radius r centered about the primary backbone. The proximal secondary backbones are superelastic NiTi tubes while the distal secondary backbones are superelastic NiTi wires that run concentrically inside the proximal backbones. The structure is bounded by stainless steel base and end disks and a multitude of spacer disks which maintain approximate radial symmetry as each segment bends. By controlling the lengths of the secondary backbones, two Degrees-of-Freedom (DoF) per segment are achieved. A review of the kinematics can be found in Simaan et al. [33].

Table I presents the kinematic parameters of each segment. L is the kinematic length defined as the bending length of each continuum segment. r defines the pitch circle radius, Fig. 3 ⑫, from the central axis to secondary backbones of each segment. The primary backbone of both segments and the secondary backbones of the distal segment are wires and therefore do not have an inside diameter. The overall outside diameter of the DDM deployed inside the bladder is 5 mm.

Referring again to Fig. 3, the base disk of the proximal

TABLE I
DIMENSIONAL SPECIFICATIONS FOR THE CONTINUUM ROBOT

Segment	Backbone	L [mm]	r [mm]	o.d. [mm]	i.d. [mm]
Proximal	Primary	30	N/A	0.30	N/A
Proximal	Secondary	30	1.725	0.6604	0.4826
Distal	Primary	25	N/A	0.30	N/A
Distal	Secondary	25	1.725	0.4064	N/A

segment is mounted to an insertion tube ⑧ that moves the structure along the axis of the resectoscope sheaths. The inner ② and outer ① resectoscope sheaths together define the introduction direction of the DDM base into the bladder.

The cross section of the DDM, Fig. 3 (Inset), extends from the distal end of the instrument to the actuation unit and provides delivery channels for instrumentation and visualization. The cross section contains three equally spaced instrument lumens of 1.8 mm diameter ⑨ and lumens for the primary ⑪ and secondary ⑩ backbones of the proximal and distal stage. A biopsy forceps ⑦ and a laser cautery fiber ⑥ are inserted into the instrumentation channels in Fig. 3.

Intravesicular visualization is provided by a flexible 1 mm diameter fiberscope, which occupies one of the instrumentation channels. The fiberscope has a 10,000 pixel fused image guide and a high numerical aperture glass light delivery fiber. The fiberscope is coupled to a CCD camera system (Toshiba IK-M44) and a frame grabber (Sensoray 2255S) for capturing frames at 60 Hz. The fiberscope system resolution was estimated by locating, at a given distance, sets of printed black lines of varying width and spacing and estimating the line width resolvable in the image presented to the operator. The spacial resolution is estimated as line widths less than 0.2 mm at a distance of 5 mm from an imaging object and less than 1.25 mm at a distance of 50 mm. Visualization with this resolution will be commented upon in section V.

2) Actuation Unit: The motion of the DDM is controlled by a compact and portable seven DoF actuation unit. The actuation unit is composed of an insertion stage and a separable continuum actuation unit, which is an iteration of the design previously introduced by Simaan et al. [33] with incorporation of force sensing capabilities. The unit provides linear motion for insertion of the DDM into the bladder and for actuation of the DDM's two continuum segments. Fig. 4 shows schematics and a photograph of the actuation unit.

Fig. 4A presents an exploded view displaying the major subassemblies of the actuation unit. The insertion stage ① drives the 6 DoF *continuum actuation unit* through a connection plate ②. The continuum actuation unit consists of three *concentric backbone actuation assemblies* ③,④,⑤ that provide motion to the secondary backbones of the continuum segments. The backbones are routed from the concentric backbone actuation assemblies through the backbone spacing cone ⑥ to the distal DDM. The manual adjustment arm ⑦ allows position and orientation adjustment of the actuation unit assembly with respect to the coupling of the resectoscope sheaths.

The equally spaced concentric backbone actuation assemblies are shown in an exploded view in 4A ③,④,⑤ and assembled into the continuum actuation unit in Fig. 4D. Each assembly actuates the coaxially located secondary backbones

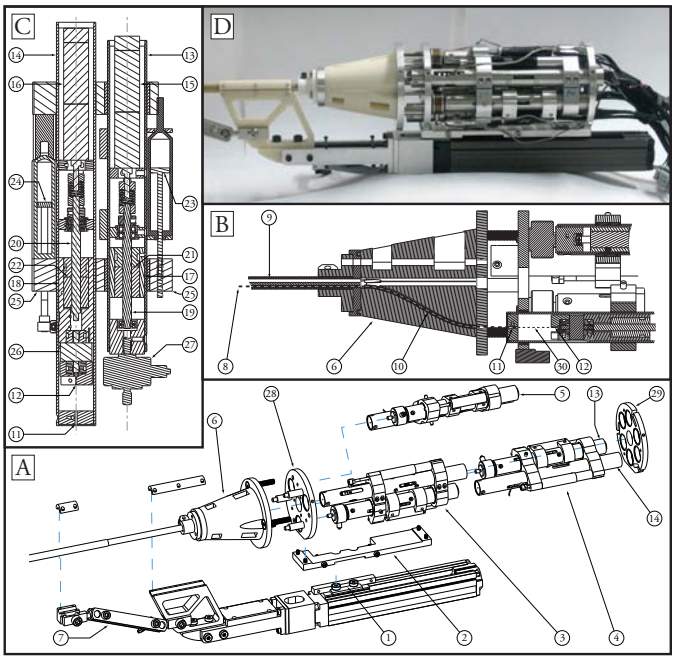

Fig. 4. Actuation unit for the telerobotic slave. (A) Exploded view with subassemblies marked. (B) path of concentric nitinol backbones guided from the distal manipulator to the backbone actuation assembly. (C) Cross section of the backbone actuation assembly. (D) Photograph of the actuation unit with cover removed. Further details in text.

of the proximal and distal continuum segments. Fig. 4C depicts a cross-section of a concentric backbone actuation assembly. The assembly is composed of a primary cylinder ⑬ and secondary cylinder ⑭. Each cylinder contains a motor ⑮⑯, driving a piston ⑰⑱, by an internal lead screw ⑲⑳. The lead screw nut inside the respective pistons ㉑㉒, is composed of two nut elements that can be tightened on the lead screw with respect to one another to remove backlash between the piston and the lead screw.

Linear motion of the piston is dually measured by motor encoders and linear potentiometers ㉓㉔ (Omega LP804-1/2). The piston in the primary cylinder is rigidly connected by shear pins to a connection arm ㉕ clamped to the outside diameter of the secondary cylinder. The secondary backbones of the proximal segment connect to the base of the secondary cylinder ⑪, thus motion of the primary cylinder piston drives the proximal secondary backbone relative to the primary cylinder. The piston of the secondary cylinder attaches through the secondary cylinder load cell ㉖ (Honeywell Model 11, 10 lbs) to the connection of the secondary backbone wire of the distal segment ⑫. This integrated load cell directly measures actuation forces in the distal secondary backbones.

Each two-cylinder concentric backbone actuation assembly (e.g. ④) connects to the base plate ㉘ of the continuum actuation unit through the primary cylinder load cell ㉗ (Honeywell Model 31, 10 lbs). As a result, the primary cylinder load cell measures the sum of the actuation forces in a set of coaxial secondary backbones attached to the assembly. To prevent moments on the primary load cell, each concentric backbone actuation assembly is supported on polymer bushings (Igus G300) at the proximal end of the primary and secondary cylinders by a top plate ㉗. Both the base and top plate connect

the continuum actuation unit through a connection plate ② to the insertion stage.

Fig. 4B illustrates the routing of the nitinol backbones from the distal section to the actuation unit. The secondary segments enter the actuation unit at the 1.725 mm kinematic radius of DDM. This radius must be expanded to a radius of 23 mm from the central axis of the continuum actuation unit for attachment to the actuation cylinders. The path of the proximal and distal secondary backbones is depicted by the dashed line ⑧ which connects with the continuum segments distally. A multi-lumen polytetrafluoroethylene (PTFE) extruded tube ⑨ supports the backbones along the length of the shaft. The concentric secondary backbones are guided through lumens of cone assembly ⑥ lined by PTFE tubing ⑩ to reduce friction. The proximal secondary backbone (labeled by ⑧ with the distal secondary backbone running concentrically within) and distal secondary backbone ㉚ attach to the actuation cylinder assembly at ⑪ and ⑫ respectively.

The actuation unit controls motion of the intravesicular DDM through the coordinated actuation of the secondary backbones of the continuum segments. An explanation of the kinematic control can be found in Simaan et al. [33]. With this control structure, benchtop evaluation of the capabilities of the system are evaluated.

IV. Evaluation of Positioning Control

In order to evaluate the overall positioning capabilities of the system in the context of a surgical application, a path tracking experiment was conducted to position and orient a laser under telemanipulation control. The experimental setup for the telerobotic evaluation is presented in Fig. 5. The system is operated in a master-slave configuration such that position commands and orientation commands were issued to the slave by an operator controlling a Sensable Phantom Omni running on a Windows 7 machine. Commands were sent across a local area network using the network User Datagram Protocol (UDP) at a nominal communication frequency of 125 Hz. The slave actuation unit was controlled by the Matlab xPC real-time operating system running an inverse kinematics algorithm and joint level PID control at 1 kHz. Position commands from master to slave were scaled 5:1 and orientation commands were not scaled. Bajo et al. [**?**] offers a complete description of the telemanipulation architecture over UDP.

Path tracking error of a laser point serves as a metric for evaluating the manipulation capabilities of the surgical slave. Control of a projected laser source is directly related to the clinical task of controlling laser fibers delivering energy from a high powered laser source during TURBT as will be introduced in section V. A 5 mW red laser diode was rigidly attached to the end disk of the DDM of the surgical slave with a fuse deposition manufacturing adapter, Fig. 5. The laser pointer was modified to reduce weight by substituting wired power for the batteries and removing its outer housing. A sheet of printer weight paper was positioned in front of the surgical slave at a distance of approximately 2 to 3 cm. The distance is approximate because the experimental setup and telerobotic control allows adjustment of the distance from the distal end

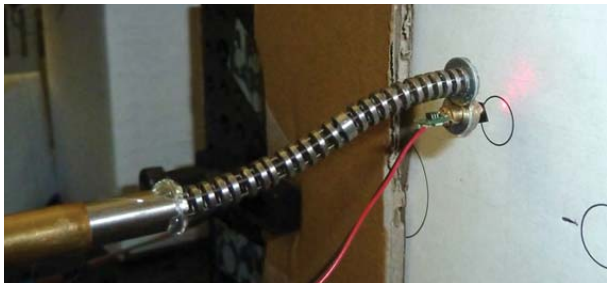

Fig. 5. Experimental setup for the telemanipulation path tracking experiment. Users direct a laser spot on a target screen via a master interface controlling the surgical slave system.

of the DDM to the paper. A circle of 10 mm was printed on the side of the paper oriented toward the surgical slave and ruled lines were printed on the opposite side. Six users, including four graduate research assistants, a faculty member of the mechanical engineering department, and a urologic surgeon, were presented with the task of tracing this circle with the spot of the laser projected onto a paper for five revolutions. Video of the path tracking was recorded on the opposite side of the paper with a commercial video camera.

Still frames extracted from the recorded videos were individually analyzed via an automatic algorithm to generate the path tracking error over each trial. The frames were segmented for the location of the center of the laser spot, via standard image segmentation algorithms [34], and estimation of the distance to the closest point on the circle. For individual frames, the tracking error was determined as the distance from the current center point of the laser to the closest point on the circle.

To evaluate the quality of the automatic segmentation algorithm, the center position estimates from a single trial were compared to estimates of the laser center generated manually in each frame. Over the total of 183 frames of the trial, the mean error between the algorithm and manual identification was 0.16 mm with a standard deviation of 0.08 mm. The maximum error over the sequence was 0.39 mm. Thus the automatic segmentation algorithm is suitable for generating results with submillimetric accuracy.

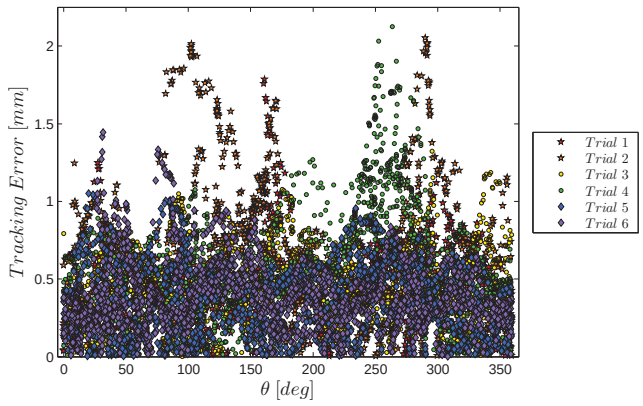

Fig. 6. Path tracking errors for the telemanipulation trials as a function of orientation with respect to the closest point on the target path circle

Results of the telemanipulation study are presented in Fig. 6. The figure displays the tracking error for the segmented frames of each trial as a function of the orientation to the closest point on the path circle where 0° corresponds to the top of the circle. The mean tracking error across all subjects was 0.48 mm with a standard deviation of 0.31 mm. A maximal tracking error of 2.12 mm occurred in trial 4. With the exception of the Vanderbilt authors, marked Trials 1 and 3, users had no prior experience or training with the teleoperation system. Note that the accuracy for the majority of the users was within 0.5 mm RMS error. The results confirm precise telemanipulation is achievable with the prototype surgical slave system. Further improvement to the scaling of the master interface and mechanical components in the slave robot, including replacing the lead screws with ball screws and closing backlash, are expected to further improve this precision. We believe that the achieved submillimetric performance is sufficient for accurate resection that can be systematized throughout a cohort of trained operators.

V. Evaluation of Surveillance and Intervention

Multimedia extension I shows videos of the various experiments reported in this section. The system was deployed in an ex-vivo bovine bladder to analyze the function and performance under clinically realistic conditions. The experimental conditions are illustrated in Fig. 7. The telerobotic surgical system ③ is deployed through a standard resectoscope ② into an ex-vivo bovine bladder ①. As specified in the previous section, the DDM is controlled by a Sensable Phantom Omni ⑤. The end-effector view through the fiberscope is displayed to the user on the master console ④. A laparoscope ⑥ is additionally deployed for insufflation of the bladder and visualization of the DDM. Indigo blue dye was manually injected into the bladder wall with a syringe to define the eleven target areas in anterior, posterior, superior, inferior, right and left sections of the bladder.

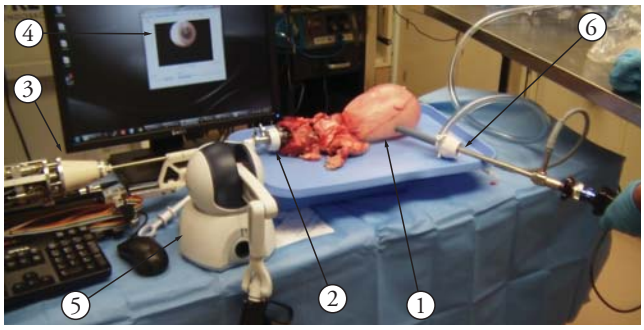

Fig. 7. Overview of the ex-vivo bovine bladder experimental setup

Fig. 8 displays subsequent images as the DDM deploys into the bladder and moves within to visualize sections of the bladder urothelium based on operator commands. The operator first manipulated the DDM to visualize each section of the bladder. A 0.55 mm diameter probe encasing a 200 μm diameter holmium laser fiber was subsequently deployed through one of the access channels. The slave was then manipulated to cauterize the 9 of the 11 labeled tissue areas using laser energy on the target areas as shown in Fig. 9 (Left). The bladder urothelium after laser delivery is shown in Fig. 9 (Right).

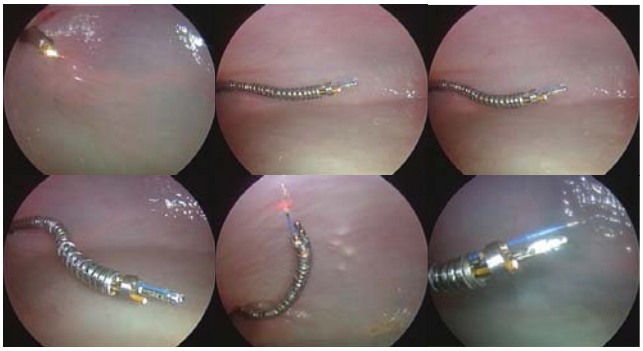

Fig. 8. Photographs of the DDM deployment through the resectoscope sheath and subsequent movement for surveillance.

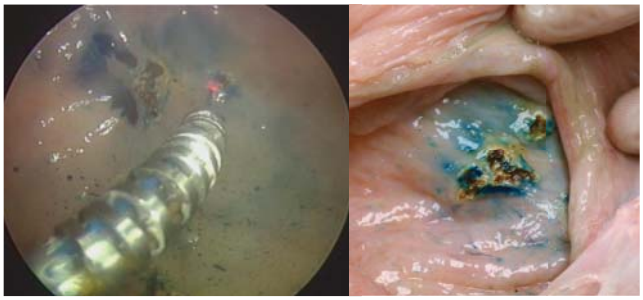

Fig. 9. Laser cauterization of ex-vivo bovine bladder. (Left) Laparoscope view of the system delivering laser energy over a target area as defined by indigo blue dye. (Right) Clinical view of a target area after completion of the experiment.

A technique combining forceps grasping with laser energy delivery allowed gross resection of urothelium. The robot was guided to each of the remaining labeled areas. The target tissue was grasped and retracted by the forceps, Fig. 10 (Left). The DDM was subsequently maneuvered to deliver laser energy concentrically around the grasper and tissue such that a sample of the tissue was resected, Fig. 10 (Right), while leaving sufficient tissue of the muscular layer intact to preserve the integrity of the bladder.

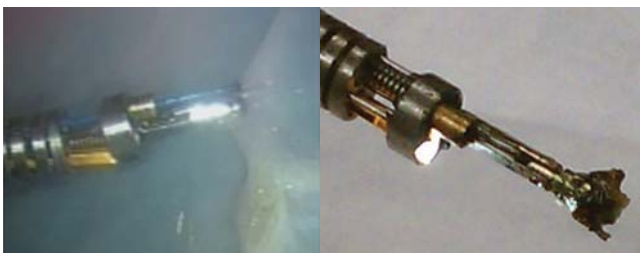

Fig. 10. Deployment of biopsy forceps. (Left) Laparoscope view of the system grasping bladder urothelium with a biopsy forceps and delivering parallel laser energy. (Right) Clinical view of a sample removed with combined grasping and laser delivery.

The experiment demonstrated the function of the robot to navigate and intervene in clinical conditions and highlighted a limitation of the initial prototype. The system was capable of effective surveillance, energy delivery and performance complex multi-instrument procedures. The main limitation of the system is the on-board $\varnothing$ 1 mm fiberscope prototype with embedded light source. Both the amount of light and resolution limited the usefulness of the onboard view and required additional visualization from the external laparoscope. The limited cross section requires a tradeoff between fibers used for visualization and fibers used for illumination. Although, the fiberscope was effective for examination of tissue and maneuvering the end-effector locally on the tissue, the poor distance resolution was insufficient for gross motion. Thus, a resolution of 1.25 mm at a distance of 50 mm is insufficient as a complete replacement for the current resectoscope lens and camera. The modular design of the system, with multiple instrument ports, will allow iterative improvement to the imaging without changes or redesign of the overall system.

VI. Conclusions

Treatment of urinary bladder tumors presents both a unique challenge and opportunity due to the direct access through the urethra. Comprehensive and reliable MIS staging resection and treatment of bladder lesions is limited by the current state-of-the-art instrumentation. The rigid resectoscope lacks the intravesicular maneuverability to provide consistent tumor resection. Despite the significant patient morbidity and mortality caused by bladder cancer and the interest of clinical and engineering investigators to improve patient outcomes, no platform exists for development and standardization of novel techniques for TURBT.

This work has presented a novel telerobotic system for minimally invasive bladder surveillance and surgical intervention. Features of the design include an intravesicular dexterous manipulator, multiple instrumentation channels for a diverse set of tools and compatibility with current resectoscope sheaths in a compact system. A telerobotic path tracking experiment evaluated the suitability of the system for non-linear intravesicular tracking tasks such as bladder urothelium surveillance and delivery of laser energy for cautery. Submillimetric RMS positioning error was achieved during tracking of a non-linear target path with a laser mounted to the slave system. This setup mimicked the clinical task of laser cautery during TURBT. An ex-vivo study of the system deployed in a bovine bladder demonstrated the utility of the system for surveillance and energy delivery under clinical conditions.

The prototype surgical slave represents an advancement toward systemizing novel techniques in TURBT with the goal of improving patient outcomes in bladder cancer. Future testing of the system will integrate real-time parallel imaging technologies and evaluate performance in in-vivo models. The authors believe improvement in the positioning accuracy and intravesicular dexterity, coupled to novel imaging and telerobotic control will facilitate the development and systematization of new techniques for reduction in complications and recurrence in NMIBC.

References

[1] R. Siegel, D. Naishadham, and A. Jemal, "Cancer statistics, 2012." *CA: A Cancer Journal for Clinicians*, vol. 62, no. 1, pp. 10–29, 2012.

[2] L. Cheng, R. Montironi, D. D. Davidson, and A. Lopez-Beltran, "Staging and reporting of urothelial carcinoma of the urinary bladder," *Modern Pathology*, vol. 22, no. S2, pp. S70–95, Jun. 2009.

[3] H. W. Herr and S. M. Donat, "Quality control in transurethral resection of bladder tumours," *BJU International*, vol. 102, no. 9 Pt B, pp. 1242–6, Nov. 2008.

[4] E. C. C. Cauberg, D. M. de Bruin, D. J. Faber, T. G. van Leeuwen, J. J. M. C. H. de La Rosette, and T. M. de Reijke, "A new generation of optical diagnostics for bladder cancer: technology, diagnostic accuracy, and future applications," *European Urology*, vol. 56, no. 2, pp. 287–96, Aug. 2009.

[5] D. Wilby, K. Thomas, E. Ray, B. Chappell, and T. O'Brien, "Bladder cancer: new TUR techniques," *World Journal of Urology*, vol. 27, no. 3, pp. 309–12, Jun. 2009.

[6] A. J. Pantuck, J. Baniel, Z. Kirkali, T. Klatte, N. Zomorodian, O. Yossepowitch, and A. S. Belldegrun, "A novel resectoscope for transurethral resection of bladder tumors and the prostate," *The Journal of Urology*, vol. 178, no. 6, pp. 2331–6, Dec. 2007.

[7] P. Babbar and A. K. Hemal, "Robot-assisted urologic surgery in 2010 - Advancements and future outlook." *Urology Annals*, vol. 3, no. 1, pp. 1–7, Jan. 2011.

[8] A. A. Goldenberg, J. Trachtenberg, W. Kucharczyk, Y. Yi, M. Haider, L. Ma, R. Weersink, and C. Raoufi, "Robotic System for Closed-Bore MRI-Guided Prostatic Interventions," *IEEE/ASME Transactions on Mechatronics*, vol. 13, no. 3, pp. 374–379, Jun. 2008.

[9] J. Tokuda, G. S. Fischer, S. P. DiMaio, D. G. Gobbi, C. Csoma, P. W. Mewes, G. Fichtinger, C. M. Tempany, and N. Hata, "Integrated navigation and control software system for MRI-guided robotic prostate interventions." *Computerized Medical Imaging and Graphics*, vol. 34, no. 1, pp. 3–8, Jan. 2010.

[10] P. C. Mozer, A. W. Partin, and D. Stoianovici, "Robotic image-guided needle interventions of the prostate." *Reviews in Urology*, vol. 11, no. 1, pp. 7–15, Jan. 2009.

[11] E. Sánchez de Badajoz, A. Jiménez Garrido, V. F. Muñoz Martínez, J. M. Gómez de Gabriel, and A. García Cerezo, "[Transurethral resection by remote control] [Article in Spanish]." *Archivos españoles de urología*, vol. 51, no. 5, pp. 445–9, Jun. 1998.

[12] E. Sánchez de Badajoz, A. Jiménez Garrido, F. García Vacas, V. F. Muñoz Martínez, J. Gómez de Gabriel, J. Fernández Lozano, and A. García Cerezo, "[New master arm for transurethral resection with a robot] [Article in Spanish]." *Archivos españoles de urología*, vol. 55, no. 10, pp. 1247–50, Dec. 2002.

[13] R. Hashimoto, K. Daeyoung, N. Hata, and T. Dohi, "A tubular organ resection manipulator for transurethral resection of the prostate," in *2004 IEEE/RSJ International Conference on Intelligent Robots and Systems (IROS) (IEEE Cat. No.04CH37566)*, vol. 4. Sendai, Japan: IEEE, 2004, pp. 3954–3959.

[14] M. Aron and M. M. Desai, "Flexible robotics." *The Urologic Clinics of North America*, vol. 36, no. 2, pp. 157–62, viii, May 2009.

[15] W. J. Yoon, S. Park, P. G. Reinhall, and E. J. Seibel, "Development of an Automated Steering Mechanism for Bladder Urothelium Surveillance," *Journal of Medical Devices*, vol. 3, no. 1, pp. 011 004–9, Mar. 2009.

[16] N. a. Maruniak, K. Takezawa, and W. M. Murphy, "Accurate pathological staging of urothelial neoplasms requires better cystoscopic sampling," *The Journal of urology*, vol. 167, no. 6, pp. 2404–7, Jun. 2002.

[17] E. C. C. Cauberg, J. J. M. C. H. de La Rosette, and T. M. de Reijke, "How to improve the effectiveness of transurethral resection in nonmuscle invasive bladder cancer?" *Current Opinion in Urology*, vol. 19, no. 5, pp. 504–10, Sep. 2009.

[18] O. Traxer, F. Pasqui, B. Gattegno, and M. S. Pearle, "Technique and complications of transurethral surgery for bladder tumours," *BJU International*, vol. 94, no. 4, pp. 492–6, Sep. 2004.

[19] L. Walker, T. G. Liston, and R. W. LLoyd-Davies, "Does flexible cystoscopy miss more tumours than rod-lens examination?" *British Journal of Urology*, vol. 72, no. 4, pp. 449–50, Oct. 1993.

[20] H. B. Grossman, M. Soloway, E. Messing, G. Katz, B. Stein, V. Kassabian, and Y. Shen, "Surveillance for recurrent bladder cancer using a point-of-care proteomic assay." *JAMA*, vol. 295, no. 3, pp. 299–305, Jan. 2006.

[21] G. Mowatt, J. N'Dow, Z. Shihua, M. Kilonzo, C. Boachie, C. Fraser, G. Nabi, J. Cook, L. Vale, and T. Griffiths, "Photodynamic Diagnosis of Bladder Cancer Compared with White Light Cystostopy," *European Urology Supplements*, vol. 8, no. 4, pp. 373–373, Mar. 2009.

[22] G. A. Sonn, S.-N. E. Jones, T. V. Tarin, C. B. Du, K. E. Mach, K. C. Jensen, and J. C. Liao, "Optical biopsy of human bladder neoplasia with in vivo confocal laser endomicroscopy." *The Journal of Urology*, vol. 182, no. 4, pp. 1299–305, Oct. 2009.
[23] J.-M. Yang and W.-C. Huang, "Bladder Wall Thickness on Ultrasonographic Cystourethrography: Affecting Factors and Their Implications," *Journal of Ultrasound in Medincine*, vol. 22, no. 8, pp. 777–782, 2003.
[24] M. Oelke, K. Höfner, U. Jonas, D. Ubbink, J. de la Rosette, and H. Wijkstra, "Ultrasound measurement of detrusor wall thickness in healthy adults." *Neurourology and urodynamics*, vol. 25, no. 4, pp. 308–17, Jan. 2006.
[25] A. H. Blatt and L. Chan, "The importance of bladder wall thickness in the assessment of overactive bladder," *Current Bladder Dysfunction Reports*, vol. 4, no. 4, pp. 220–224, Nov. 2009.
[26] M. Brausi, "Variability in the Recurrence Rate at First Follow-up Cystoscopy after TUR in Stage Ta T1 Transitional Cell Carcinoma of the Bladder: A Combined Analysis of Seven EORTC Studies," *European Urology*, vol. 41, no. 5, pp. 523–531, May 2002.
[27] R. Ukai, E. Kawashita, and H. Ikeda, "A new technique for transurethral resection of superficial bladder tumor in 1 piece," *The Journal of Urology*, vol. 163, no. 3, pp. 878–9, Mar. 2000.
[28] A. Bajo and N. Simaan, "Finding Lost Wrenches: Using Continuum Robots for Contact Detection and Estimation of Contact Location," in *Proceedings of the 2010 IEEE International Conference on Robotics and Automation*, Anchorage, AK, 2010, pp. 3666–3673.
[29] K. Xu and N. Simaan, "An Investigation of the Intrinsic Force Sensing Capabilities of Continuum Robots," *IEEE Transactions on Robotics and Automation*, vol. 24, no. 3, pp. 576–587, 2008.
[30] ——, "Intrinsic Wrench Estimation and Its Performance Index for Multisegment Continuum Robots," *IEEE Transactions on Robotics*, vol. 26, no. 3, pp. 555–561, Jun. 2010.
[31] R. E. Goldman, A. Bajo, and N. Simaan, "Compliant motion control for continuum robots with intrinsic actuation sensing," in *Proceedings of the 2011 IEEE International Conference on Robotics and Automation*. IEEE, May 2011, pp. 1126–1132.
[32] A. J. Wein, L. R. Kavoussi, A. C. Novick, A. W. Partin, and C. A. Peters, *Campbell-Walsh Urology*, 9th ed. Philadelphia: W.B. Saunders, 2007.
[33] N. Simaan, K. Xu, A. Kapoor, W. Wei, P. Kazanzides, P. Flint, and R. Taylor, "Design and Integration of a Telerobotic System for Minimally Invasive Surgery of the Throat." *The International Journal of Robotics Research*, vol. 28, no. 9, pp. 1134–1153, Sep. 2009.
[34] R. C. Gonzalez, R. E. Woods, and S. L. Eddins, *Digital Image Processing Using MATLAB*. Gatesmark Publishing, Sep. 2009.

Roger E. Goldman (M'07) received the B.Sc. degree in mechanical engineering from Stanford University, Stanford, CA, in 2002 and the Ph.D. degree in biomedical engineering from Columbia University in 2012. He is currently working toward the M.D. degree at the College of Physicians and Surgeons, Columbia University, New York, NY.

In 2003, he joined Foxhollow Technologies, Inc., Redwood City, CA, as a Research & Development Engineer, where he developed catheters for endovascular procedures. He is currently a National Institutes of Health (NIH) Medical Scientist Training Program Fellow at Columbia University. His research interests include novel robotic instruments for medical diagnosis and therapy.

Andrea Bajo (S'10) received the first-level *Laurea* degree in control engineering from the University of Rome La Sapienza, Rome, Italy, in 2007 and the M.Sc. degree in mechanical engineering from Columbia University, New York, NY, in 2009. He is currently working toward the Ph.D. degree with the Department of Mechanical Engineering, Vanderbilt University, Nashville, TN.

His research interests include kinematics, collision detection, estimation of constraints, dynamics, and control of continuum robots for surgical applications.

Lara S. MacLachlan received a B.Sc. degree in mechanical engineering from the Massachusetts Institute of Technology in Cambridge, MA in 1998 and a M.D. degree from the Yale University School of Medicine in New Haven, CT in 2007. She is currently undergoing her post-graduate medical training in urology at the New York Presbyterian Hospital - Columbia University Medical Center in New York, NY.

In 1998, she joined the Guidant Corporation in Santa Clara, CA as a Research & Development Engineer, where she developed catheters and coronary stents for minimally invasive cardiac procedures. In 2001, she worked as a Research Assistant in the Molecular & Cellular Biology Department of Harvard University in Cambridge, MA.

Dr. MacLachlan is a member of the American Urological Association.

Ryan Pickens received the M.D. degree from the University of Louisville College of Medicine in 2006. He completed residency in Urologic Surgery in 2011.

He is currently an Endourology/Minimally Invasive Fellow at the Vanderbilt University Medical Center, Nashville, TN. Current research includes collaborative development of image-guided minimally invasive and robotic surgery for kidney and abdominal organs with Biomedical Engineering, new robotic platform development with Mechanical Engineering, and magnetic camera technologies.

S. Duke Herrell received a M.D. degree from the University of Virginia School of Medicine, Charlottesville, VA in 1990. He completed residency in Urologic Surgery in 1996, and a fellowship in Minimally Invasive Urologic Surgery at Loyola University Medical Center in 1997.

He joined Vanderbilt University in 2001 to direct minimally invasive urologic surgery and robotics and where he is currently an Associate Professor of Urologic Surgery and Biomedical Engineering. Current research includes collaborative development of image-guided minimally invasive and robotic surgery for kidney and abdominal organs and a variety of cutting edge technology developments including NIR fluorescent tumor tags and optical tissue interrogation. Dr. Herrell is also a busy clinical surgeon specializing in kidney and prostate cancer and urinary reconstruction. He has been an invited plenary speaker on robotics, engineering, and the future of surgery at the SPIE Engineering meeting 2011 and the American Urologic Association 2011.

Dr. Herrell is a Fellow of the American College of Surgeons and a member of Society of Urologic Oncology, American Urological Association, Endourological Society and Society of Laparoendoscopic Surgeons.

Nabil Simaan (M'04) received a mechanical engineering Ph.D. in 2002 from the TechnionIsrael Institute of Technology, Haifa, Israel. From 2003-2004, he was a Postdoctoral Research Scientist with National Science Foundation (NSF) Engineering Research Center for Computer-Integrated Surgical Systems and Technology, Johns Hopkins University, Baltimore, MD, where he was involved in research on minimally invasive robotic assistance in confined spaces. In 2005, he joined Columbia University, New York, NY, as an Assistant Professor of mechanical engineering and the Director of the Advanced Robotics and Mechanisms Applications Laboratory. He was promoted to Associate Professor in 2010. He has been with the Department of Mechanical Engineering at Vanderbilt University since the Fall semester of 2010. Dr. Simaan received the NSF Career award for young investigators to design new algorithms and robots for safe interaction with anatomy in 2009.